Kinetics of the reduction of pinacolone by borane–dimethyl sulfide and catecholborane in THF

Conrad Eckhardt, Holger Jockel and Reinhard Schmidt*

*Institut für Physikalische und Theoretische Chemie, J. W. Goethe-Universität,
Marie-Curie-Str. 11, D60439 Frankfurt/M, Germany*

Received (in Cambridge, UK) 21st April 1999, Accepted 23rd July 1999

The kinetics of the reduction of the ketone, pinacolone by borane–dimethyl sulfide and catecholborane have been investigated in tetrahydrofuran. Both overall reactions are composed of several subsequent and in part competing reactions. The use of commercial borane–dimethyl sulfide results in fast reactions and the borane reaction order of 1.6. In contrast, purified borane–dimethyl sulfide reacts distinctly slower and yields very different kinetics. The main reaction, the reduction of the ketone by the borane–dimethyl sulfide complex forming the monoalkoxyborane, is first order in both reactants similar to the reduction of pinacolone by the borane–tetrahydrofuran complex. The overall reaction with catecholborane proceeds much slower and appears to be much more complex. The reaction order is two in catecholborane and zero in ketone. Obviously, the reactive intermediates are derived from dimeric species of catecholborane. The kinetics of both different types of reaction can successfully be simulated by numerical integration. The results obtained from the evaluation of the kinetics are complemented by semi-empirical calculations in order to characterize the possible intermediates.

Introduction

The enantioselective reduction of prochiral ketones by borane reagents catalyzed by chiral oxazaborolidines has generated great interest because of its many synthetic uses.[1–6] Interestingly, despite its importance there exists almost no kinetic studies on this type of reaction. Recently, we published the first investigations of the direct reaction and the oxazaborolidine (OAB) catalyzed reduction of the ketone pinacolone by the borane–tetrahydrofuran (B–T) complex in tetrahydrofuran (THF).[7,8] The actual catalytic cycle competes with the direct reduction of the ketone by the borane reagent. Therefore, detailed knowledge of the reaction kinetics of the direct reduction is very important for a systematic optimization of the overall catalytic process. The direct reduction of prochiral ketones produces no enantiomeric excess. Thus, highly reactive borane reagents could lead to low ee values. This is the reason why alongside B–T the less reactive reagents borane–dimethyl sulfide (B–D)[9–11] and catecholborane (CB)[12–15] have also been used in the OAB catalyzed reduction of ketones. Since kinetic studies with these reagents have not yet been reported, we extended our investigations and report in this work the results on the kinetics of the direct reduction of pinacolone (P) in THF by B–D and CB, respectively.

Results and discussion

Reactivity of borane–dimethyl sulfide in THF

In our previous investigation of the direct reduction of P by B–T we observed very different reaction rates and kinetics, if we used freshly prepared, pure B–T rather than commercial B–T as the reducing agent.[7] There have been similar findings in the present study with B–D. Fig. 1 plots the decrease of the absorbance of P at 20 °C. Although the same overall concentrations were used ($[\mathrm{P}]_o = 0.1$, $[\mathrm{B{-}D}]_o = 0.5$ mol dm^{-3}), we observed again very different reaction kinetics.

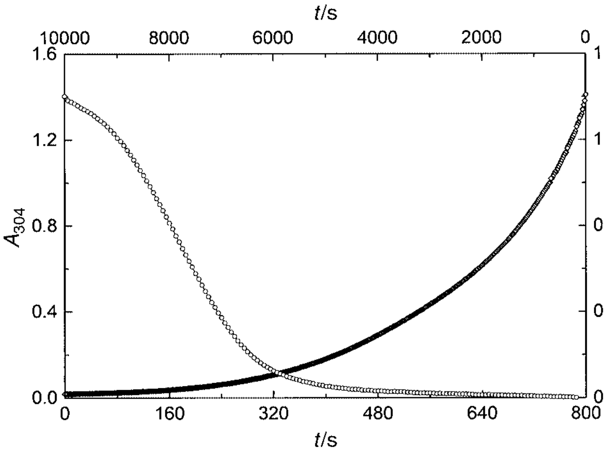

Fig. 1 Kinetic traces of the reduction of P with $[\mathrm{B{-}D}]_o = 0.50$ mol dm^{-3} and $[\mathrm{P}]_o = 0.10$ mol dm^{-3}, A_{304} is the absorbance at 304 nm. Lower time scale: (○) with commercial B–D. Upper reversed timescale: (◇) with purified B–D.

With commercial B–D some autocatalytic process is operating. Half of P is consumed after $\tau_{1/2} = 180$ s. A kinetic curve of very similar form but a much faster reaction ($\tau_{1/2} = 6$ s) was found under the same experimental conditions for the direct reduction of P by commercial B–T.[7] The reaction of the purified B–D with P is distinctly slower ($\tau_{1/2} = 1600$ s) and without initial acceleration. Furthermore, we observed peculiarites with respect to the borane reaction order (RO). For commercial B–T we found the surprising value of RO = 1.6, whereas RO = 1 was determined for purified B–T.[7] For the commercial B–D we now measured from the variation of $\tau_{1/2}$ with $[\mathrm{B{-}D}]_o$ the unusual value of RO = 1.6 (plot not shown). The enhanced reactivity of the commercial B–T is principally caused by the catalyzing effect of $NaBH_4$, which is added as a stabilizer of B–T.[7] It may be speculated that similar impurities cause the enhanced reactivity of commercial B–D. In the further study we only used purified B–D. It has to be noted that under the same experimental conditions the reactivity of the purified B–D still varied from sample to sample by about ±15%.

Kinetics of the reduction with borane–dimethyl sulfide

Since two hydride equivalents of B–T or B–D are readily

Table 1 Dependence of the pseudo-first-order rate constant k_{p1} of the reduction of P on $[B–D]_o$; dependence of the reaction rate r of the reduction of P on $[CB]_o$

$[B–D]_o/dm^3\ mol^{-1}$	$k_{p1}/s^{-1\,a}$	$[CB]_o/dm^3\ mol^{-1}$	$r/mol\ dm^{-3}\ s^{-1\,a}$
0.064	9.5×10^{-5}	0.50	1.4×10^{-7}
0.102	1.8×10^{-4}	1.00	5.9×10^{-7}
0.249	2.9×10^{-4}	1.50	2.4×10^{-6}
0.500	4.0×10^{-4}	2.00	3.5×10^{-6}
1.000	8.1×10^{-4}	2.50	6.8×10^{-6}
1.972	2.8×10^{-4}	3.00	8.9×10^{-6}
		3.50	1.2×10^{-5}

[a] Experimental uncertainty ±15%.

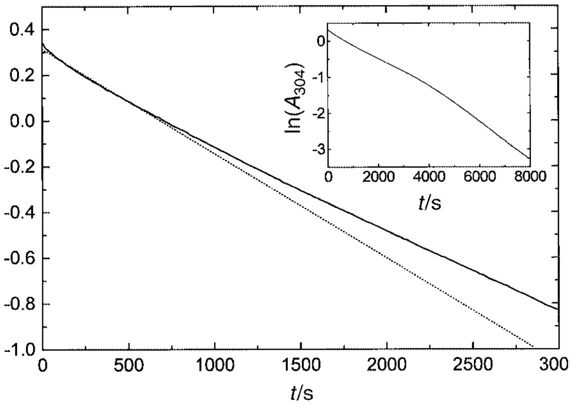

Fig. 2 Deviation of the reaction from monoexponential behaviour, $[P]_o = 0.10$ mol dm^{-3}; $[B–D]_o = 0.50$ mol dm^{-3}. Straight line represents monoexponential fit to the first 25% conversion of P, $k_{p1} = 4.6 \times 10^{-4}$ s^{-1} at 20 °C. Inset, kinetic curve on an extended timescale.

available for the reaction with ketones,[9,16,17] the experiments of Fig. 1 with $[P]_o = 0.1$ and $[B–D]_o = 0.5$ mol dm^{-3} correspond almost to pseudo-first-order conditions. Nevertheless, the decrease of P in the reaction with the purified B–D differs distinctly from a monoexponential decay, as can be seen from the semilogarithmic representations of Fig. 2.

The straight line is the result of the linear least squares fit to the data between 20 s and 640 s, *i.e.*, during the first 25% of conversion of P. The decrease of [P] in that interval amounts to 0.025 mol dm^{-3}. Therefore, $[B–D]_o = 0.5$ mol dm^{-3} is nearly constant and the slope represents the overall pseudo-first-order rate constant $k_{p1} = 4.6 \times 10^{-4}$ s^{-1} at 20 °C. The experimental curve is steeper at the beginning of the reaction. The reason for this fast initial reaction, which contributes to the overall reaction with the small conversion of $\Delta[P] \approx 0.01[P]_o$, is not known. A very similar effect had already been observed in the reaction with B–T.[7] As is shown by the inset of Fig. 2 the slope d ln A_{304}/dt gets steeper again after about 4000 s or 80% conversion of P. A similar but smaller deviation to larger rates was observed for the reaction of P with B–T and is in part most probably caused by some catalyzing effect of the alkoxyborane produced. The deviations of the experimental kinetic curves from monoexponentiality shown in Fig. 2 are typical and have been found in all experiments.

Further reactions with $[P]_o = 0.1$ mol dm^{-3} but varying $[B–D]_o$ have been performed, to determine the reaction order in B–D. Data of k_{p1} have been evaluated considering the absorbance data only up to the following conversions of P at $[B–D]_o$: 6% at 0.064 mol dm^{-3}, 10% at 0.10 mol dm^{-3}, 15% at 0.25 mol dm^{-3}, 50% at 1.0 mol dm^{-3}, and 70% at 1.97 mol dm^{-3}. The data of k_{p1} are listed in Table 1. Fig. 3 gives the double logarithmic plot of k_{p1} *vs.* $[B–D]_o$.

A linear correlation of the data with slope 0.9 ± 0.1 results, demonstrating that the main reaction of the reduction of P is also first order in B–D. Thus, we notice a second marked difference between the reaction kinetics observed with commercial and with purified B–D: the catalytic activity of the impurities of the commercial B–D varies the reaction order in borane from 1 to about 1.6. Obviously, the mechanism of the reduction and in consequence the reaction rate changes distinctly.

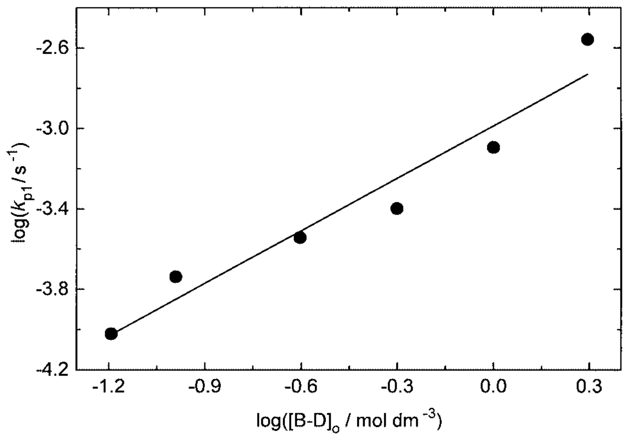

Fig. 3 Determination of the B–D reaction order: (●) experimental data; straight line represents fit, RO = 0.9 ± 0.1.

Kinetic scheme

For the interpretation of the kinetics of the consumption of P we have to consider the results of studies on the product distribution as well as our previous kinetic results with B–T. Dialkoxyboranes (DB) are the principal reaction products formed in the borane reduction of ketones.[16,17] Monoalkoxyboranes (MB) are rapidly removed by the reactions with ketone or with MB to yield DB.[17,18] The rate constants of these reactions in THF at 20 °C are already known for the ketone P from our previous study.[7] Trialkoxyborane and borane are produced in a much slower redistribution reaction of dialkoxyboranes.[17,19] With increasing steric demand this reaction becomes much slower. If the alkoxy group is *tert*-butoxy, the equilibrium is reached in THF only after more than one month at 25 °C.[19] Therefore, the redistribution of DB = bis(3,3-dimethylbutan-2-oxy)borane can be neglected on the short timescale of the reaction of P.

Semi-empirical calculations suggest that MB and DB, like borane, coordinate with a solvent molecule to form the complexes MB–T and DB–T in THF. The oxygen atom of the ketone couples to the boron atom in the reaction with the borane reagents. It was shown that the first step of the reaction of P with B–T most probably proceeds *via* the nucleophilic substitution of T by P forming P–B with a fourfold coordinated boron atom. A one-step reaction of P with B–T to form the monoalkoxyborane–THF complex MB–T is highly improbable, since it demands a complex P–B–T with a fivefold coordinated boron atom as intermediate.[7] If we transfer these results to the reaction of P with B–D, the first step of reaction (R4), the formation of MB–T, is given by (R4.1), where D stands for dimethyl sulfide and $k_{4.1}$ for the corresponding rate constant.

$$\text{B–D} + \text{P} \longrightarrow \text{P–B} + \text{D} \quad k_{4.1} \qquad \text{(R4.1)}$$

The second step (R4.2) is the subsequent hydride shift yielding MB with a threefold coordinated boron. MB coordinates in the third step (R4.3) with a suitable base, which could be either T or D, to compensate for its electron deficit. Since the concentration [T] = 12.3 mol dm^{-3} of the solvent THF is much larger than $[P]_o$, it is assumed that MB–T is formed.

$$\text{P–B} \longrightarrow \text{MB} \quad k_{4.2} \qquad \text{(R4.2)}$$

$$\text{MB} + \text{T} \longrightarrow \text{MB–T} \quad k_{4.3} \qquad \text{(R4.3)}$$

The value of k_{1p} depends linearly on $[B\text{–}D]_o$, see also Fig. 3. Since the reaction rate of P is directly proportional to $[B\text{–}D]_o$ only for step (R4.1), it is strongly indicated that (R4.1) is the rate determining step in the sequence (R4.1) to (R4.3). Thus, the overall formation reaction of MB–T can be written as (R4). As was found in the investigation of the reduction of P by B–T, reactions (R2) and (R3) remove the intermediate MB–T.

$$\text{B–D} + \text{P} + \text{T} \longrightarrow \text{MB–T} + \text{D} \quad k_4 \qquad (R4)$$

$$\text{MB–T} + \text{P} \longrightarrow \text{DB–T} \quad k_2 \qquad (R2)$$

$$\text{MB–T} + \text{MB–T} \longrightarrow \text{DB–T} + \text{B–T} \quad k_3 \qquad (R3)$$

Reaction (R2) represents an autocatalytic branch of the overall reaction, (R3) is a redistribution reaction. Since in (R3) the borane reagent B–T is formed, finally also reaction (R1) of the reduction of P by B–T has to be included in the kinetic scheme. The principal steps of the direct reduction of P by B–D are graphically represented in Scheme 1.

$$\text{B–T} + \text{P} \longrightarrow \text{MB–T} \quad k_1 \qquad (R1)$$

Numerical integration

Eqns. (1) to (5) hold for the reaction rates of reactants and

$$d[\text{B–D}]/dt = -k_4[\text{B–D}][\text{P}][\text{T}] \qquad (1)$$

$$d[\text{P}]/dt = -k_4[\text{B–D}][\text{P}][\text{T}] - k_1[\text{B–T}][\text{P}] - k_2[\text{MB–T}][\text{P}] \qquad (2)$$

$$d[\text{MB–T}]/dt = k_4[\text{B–D}][\text{P}][\text{T}] + k_1[\text{B–T}][\text{P}] - k_2[\text{MB–T}][\text{P}] - 2k_3[\text{MB–T}]^2 \qquad (3)$$

$$d[\text{DB–T}]/dt = k_2[\text{MB–T}][\text{P}] + k_3[\text{MB–T}]^2 \qquad (4)$$

$$d[\text{B–T}]/dt = -k_1[\text{B–T}][\text{P}] + k_3[\text{MB–T}]^2 \qquad (5)$$

intermediates, whereby [I] represents the actual concentration of species I at reaction time *t*.

We have performed kinetic experiments on the reduction of P by B–D in the concentration ranges $0.016 \le [P]_o \le 0.10$ mol dm^{-3} and $0.064 \le [B\text{–}D]_o \le 1.97$ mol dm^{-3}. Since the molarity of THF was much larger than the overall concentration $[B\text{–}D]_o$, $[T] = 12.3$ mol dm^{-3} is set constant. The balanced equations relating $[B\text{–}D]_o$ and $[P]_o$ with the actual concentrations of the four different species derived from borane and pinacolone, are given by eqns. (6) and (7).

$$[\text{B–D}]_o = [\text{B–D}] + [\text{MB–T}] + [\text{DB–T}] + [\text{B–T}] \qquad (6)$$

$$[\text{P}]_o = [\text{P}] + [\text{MB–T}] + 2[\text{DB–T}] \qquad (7)$$

The following initial concentrations hold true at $t = 0$: $[\text{MB–T}]_i = 0$, $[\text{DB–T}]_i = 0$, $[\text{B–T}]_i = 0$, and $[\text{B–D}]_i = [\text{B–D}]_o$. The relatively rapid initial reaction of P with the small conversion of $\Delta[P]/[P]_o \approx 0.01$ was considered by setting $[P]_i = [P]_o - \Delta[P]$. The actual concentration of P is known at any time *t*. The rate constants of reactions (R1), (R2) and (R3) had already been determined in our previous study on the reduction of P by B–T as $k_1 = 0.0037 \pm 0.0006$ dm^3 mol^{-1} s^{-1}, $k_2 = 0.003 \pm 0.001$ dm^3 mol^{-1} s^{-1} and $k_3 = 0.2 \pm 0.1$ dm^3 mol^{-1} s^{-1} at 20 °C.[7] The system of differential eqns. (1) to (5) was solved by numerical integration considering eqns. (6) and (7), taking an estimate for k_4 and keeping the mean values of k_1, k_2 and k_3 constant. Hereby, eqns. (1) to (5) with concentrations of B–D, P, MB–T, DB–T, and B–T at $t = 0$ were multiplied with the constant time interval Δt between the consecutive reaction spectra to obtain the corresponding concentration changes Δ[B–D], Δ[P], Δ[MB–T], Δ[DB–T], and Δ[B–T], which were added to the respective concentrations to obtain the values of [B–D], [P], [MB–T], [DB–T], and [B–T] at $t + \Delta t$. The complete development of the concentrations of the reactants, products and intermediates could be derived by repetition of this procedure over the total reaction time. The program was included in a worksheet allowing for graphical comparison of the calculated and experimental decays of P. The only fitted parameter, which was varied until the calculated decrease of [P] matched the experimental decay, is k_4. The whole set of experimental kinetic curves can be reproduced by this procedure with $k_4 = (7.6 \pm 2.0) \times 10^{-5}$ dm^6 mol^{-2} s^{-1}. The standard deviation on k_4 is rather large. Its magnitude is the consequence of the changes of the reactivity of the purified B–D varying from sample to sample and the fact that we allow no uncertainty of the rate constants k_1 to k_3. The average values are fixed parameters in the evaluation procedure. Therefore, all experimental errors are collected in the uncertainty of k_4. Fig. 4 shows the results of the numerical integration for reactions with the largest excess and the smallest excess of B–D. Both reactions are very well simulated by the numerical integration, supporting the validity of the kinetic scheme (R1) to (R4).

Rate determining reaction

Only reaction (R4) is first order in B–D. Therefore, it is clearly this reaction, which is most important for the overall reduction of P in the presence of an excess of B–D. Actually, if the different reaction channels contributing to the consumption of P are

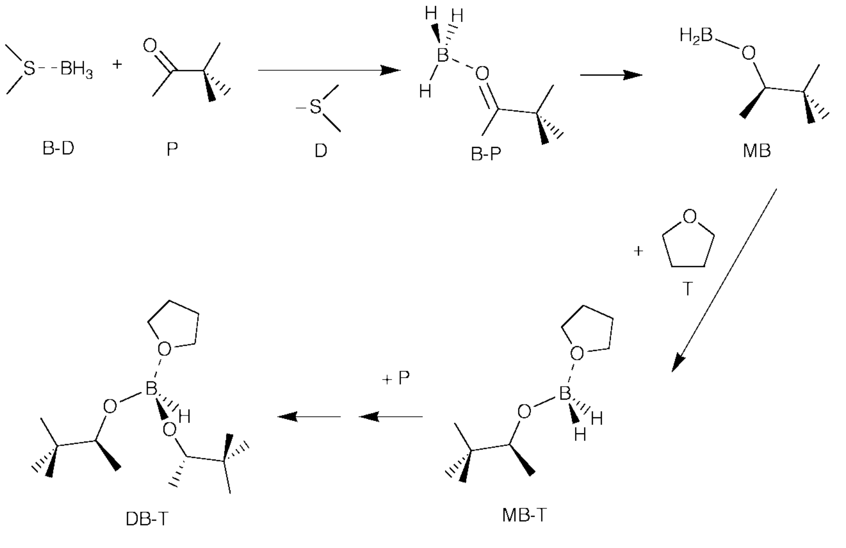

Scheme 1

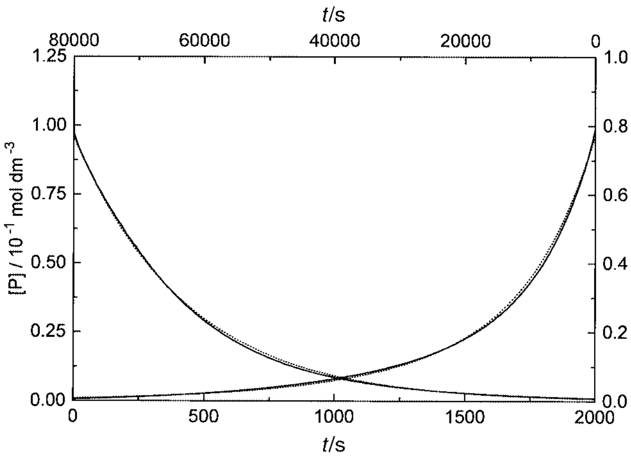

Fig. 4 Experimental and calculated kinetic curves. Solid curves represent experiment, dashed curves calculations. Concentrations in mol dm^{-3}, rate constants k_1 to k_3 in dm^3 mol^{-1} s^{-1}. $k_1 = 0.0037$, $k_2 = 0.003$, $k_3 = 0.2$. Lower timescale: $[\text{B–D}]_o = 1.97$, $k_4 = 9.4 \times 10^{-5}$ dm^6 mol^{-2} s^{-1}. Upper reversed timescale: $[\text{B–D}]_o = 0.064$, $k_4 = 8.9 \times 10^{-5}$ dm^6 mol^{-2} s^{-1}.

analyzed by numerical integration, see eqn. (2), it is found that at $[\text{P}]_o = 0.1$ mol dm^{-3} and $[\text{B–D}]_o = 0.5$ mol dm^{-3} about 90% of the total conversion of P occurs *via* reaction (R4). In fact, a mean value of $k_{1p}/([\text{B–D}]_o[\text{T}]) = (7.4 \pm 1.9) \times 10^{-5}$ dm^6 mol^{-2} s^{-1}, was obtained for the overall reaction in a large number of experiments, which agrees very well with $k_4 = (7.6 \pm 2.0) \times 10^{-5}$ dm^6 mol^{-2} s^{-1} obtained by numerical integration.

Temperature dependent kinetic experiments of the reduction of P have been performed with $[\text{P}]_o = 0.1$ mol dm^{-3} and $[\text{B–D}]_o = 0.5$ mol dm^{-3} between 7.2 and 27.0 °C. The resulting activation energy of $E_a = 62 \pm 10$ kJ mol^{-1} applies mainly to the rate constant k_4. The difference of the reactivities of the two borane reagents in the reduction of P can be quantified, if we calculate the pseudo-second-order rate constant $k_4[\text{T}] = 9.4 \times 10^{-4}$ dm^3 mol^{-1} s^{-1}. Compared with the second-order rate constant $k_1 = 3.7 \times 10^{-3}$ dm^3 mol^{-1} s^{-1} of the reaction of B–T with P, the value of $k_4[\text{T}]$ indicates a fourfold lower reactivity of B–D at 20 °C.

Mechanistic considerations

The reduction of P by B–T in THF could well be described by the reaction sequence (R1) to (R3), whereby reaction R1 dominates. According to our present analysis, the reduction of P by B–D in THF differs from the reduction of P by B–T only by the additional reaction (R4). However, now reaction (R4) is the most important of the overall reaction sequence. The separation of reaction (R4) into the individual steps (R4.1) to (R4.3), was performed in analogy to the separation of reaction (R1) into steps (R1.1) to (R1.3). (R1.1) describes the nucleophilic substitution of T in B–T by P, forming P–B with a fourfold coordinated boron atom.

$$\text{B–T} + \text{P} \longrightarrow \text{P–B} + \text{T} \qquad (\text{R1.1})$$

The subsequent steps (R1.2), the hydride shift yielding MB with a threefold coordinated boron, and (R1.3), the addition of THF to MB to compensate its electron deficit are identical with steps (R4.2) and (R4.3). Semi-empirical calculations using the AM1 parametrization[20] had been performed to see whether the results support such a mechanism for the formation of MB–T (= 2-*tert*-butylethoxyborane–THF) from P and B–T. Of course, reaction enthalpies are not directly related with equilibrium or even rate constants. Nevertheless, they are often used as very approximate guidelines in a mechanistic discussion. According to these calculations the least exothermic step in the formation of MB–T is the nucleophilic substitution reaction (R1.1) with $\Delta H_{1.1} = -11$ kJ mol^{-1}. The experimental finding that the overall reaction is in principal first order in both B–T and P, points additionally to step (R1.1) as the rate determining step of reaction (R1).

Table 2 Heats of formation H^F obtained by semi-empirical calculation with AM1 parametrization[20]

Species	H^F/kJ mol^{-1}	Species	H^F/kJ mol^{-1}
T	−245.2	CB	−339.2
P	−258.4	CB–T	−611.6
P–B	−224.4	TB	−711.6
MB	−361.7	TB–T	−972.2
MB–T	−633.8	CB2–T	−954.8
D	−39.6	TB–CB	−1050.5
B–D	−39.1	TB–CB–T	−1308.3

Following the AM1 calculations (for results see Table 2), the primary step (R4.1) of the reaction of B–D with P is by $\Delta H_{4.1} = 33$ kJ mol^{-1} endothermic, whereas steps (R4.2) (= (R1.2)), the hydride shift ($\Delta H_{4.2} = -137$ kJ mol^{-1}), and steps (R4.3) (= (R1.3)), the complexation of MB with T ($\Delta H_{4.3} = -27$ kJ mol^{-1}), are exothermic. These results are in line with the conclusion that (R4.1) is the rate determining step in the reduction of P by B–D, which is further supported by the experimental finding that the overall reaction is in principal first order in both B–D and P.

Therefore, the values of E_a of 62 ± 10 kJ mol^{-1} (B–D) and 54 ± 9 kJ mol^{-1} (B–T)[7] mainly correspond to steps (R4.1) and (R1.1), respectively. The larger activation energy for the reduction of P by B–D probably reflects the larger stability of B–D compared with the B–T complex. However, one has to keep in mind that the energies of the respective transition states will also be different.

Kinetics of the reduction with catecholborane

CB is a remarkably stable borane reagent, which can be distilled without decomposition.[21] Purification of the commercial CB (Aldrich 98%) demonstrated that the reagent was contaminated to varying extents with surprisingly large (up to 30 wt%) amounts of a white solid material, which remained as residue after distillation. Since the reagent is so badly defined, the comparison of the reaction kinetics of the commercial and the purified CB makes no sense. We therefore report only results obtained with purified CB.

The ^{1}H-NMR spectrum of $[\text{CB}]_o = 0.27$ mol dm^{-3} showed only one quartet at 3.5–5.5 ppm which is caused by the B–H proton of the catecholborane monomer. At $[\text{CB}]_o = 6.54$ mol dm^{-3}, an additional second quartet extending from 2.2 to 3.3 ppm is observed, which could result from some aggregated species, bound by three-center hydrogen bonds. In the ^{11}B-NMR spectra no significant difference between the diluted and the concentrated solution was observed. Therefore, it seems that the electronic situation of the boron atoms in the monomer and in the aggregates is very alike leading to very similar chemical shifts. A very weak quartet in the high field from −17.4 to −21.0 ppm is caused by NaB_2H_7 which is a remainder of the production process and cannot completely be extracted by purification methods.[22]

CB offers only one hydride equivalent for the reaction with ketones. As product of the reaction the trialkoxyborane (TB = 2-(2-*tert*-butylethoxy)-1,3,2-benzodioxaborole) is formed, which could be identified by NMR spectroscopy. Because of the similarity of CB with dialkoxyboranes, it is not surprising that the overall reactions are very slow. Therefore, larger concentrations compared with the other borane reagents had been used. The concentrations of CB and P in the experiment of Fig. 5 correspond nearly to pseudo-first-order conditions. Nevertheless, the decrease of P surprisingly follows

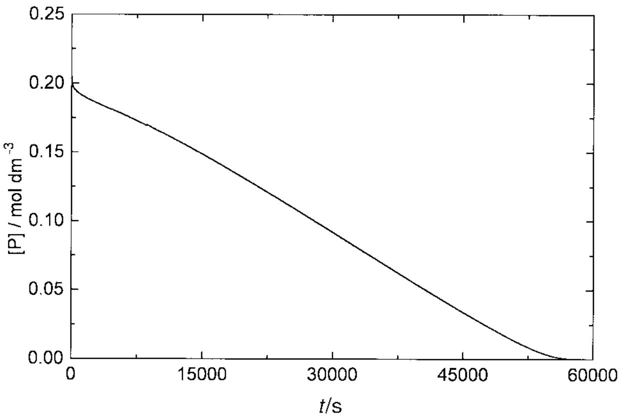

Fig. 5 Kinetic trace of the reduction of P with $[CB]_o = 2.0$ mol dm^{-3}.

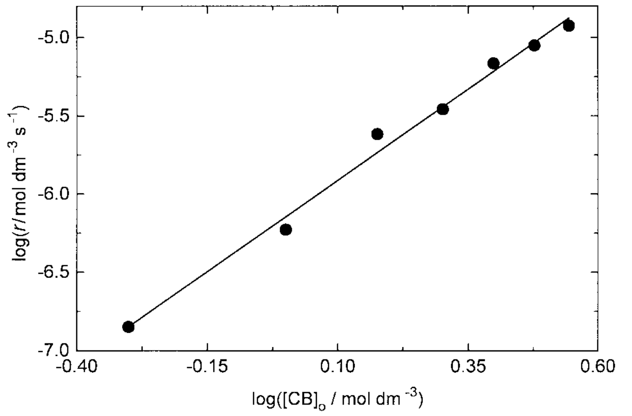

Fig. 6 Determination of the CB reaction order: (●) experimental data; straight line represents fit, RO = 2.3 ± 0.1.

almost a zero-order kinetics instead of a monoexponential decay.

The kinetic curve shown in Fig. 5 is typical for the reduction of P by CB. The inspection demonstrates a relatively rapid but small initial decay, in which the concentration decrease $\Delta[P]$ amounts to about 2 to 3% of $[P]_o$. This initial reaction could be caused by NaB_2H_7 which is present in the purified CB as a contaminant (less than 1%, by NMR). Subsequently, a wide range follows, in which the reaction rate $r = -d[P]/dt$ remains almost constant. In fact, there is a slight increase of r followed by a slight decrease. Finally, r rapidly approaches zero after about 95% consumption of P. This kinetic behavior is very particular and allows only the evaluation of reaction rates instead of rate constants. Therefore, the range of constant reaction rate directly following the initial decay was always used for evaluation.

For the determination of the reaction order in CB we investigated the reaction of $[P]_o = 0.2$ mol dm^{-3} in THF at 20 °C with $[CB]_o$ varying from 0.5 to 3.5 mol dm^{-3}. The data of r are listed in Table 1. The double logarithmic plot of r *vs.* $[CB]_o$ is given in Fig. 6.

The linear least squares fit of the data results in slope 2.3 ± 0.1, indicating that the main reaction of the reduction of P is second-order in CB and zero-order in P, see Fig. 5. Thus, we notice very strange kinetics with CB, very different from the reactions with B–T and B–D.

Kinetic scheme

The reaction order of two in CB undoubtedly requires the consideration of a dimeric CB species as the reactive intermediate. However, only at very high concentrations of CB is a second quartet observed in the ^{1}H-NMR spectrum, which could result from a dimeric species CB2. Therefore, CB2 can only be present in rather low equilibrium concentrations. The reaction order of zero in P points to some autocatalytic character of the reaction and a bottleneck in the reaction flow. Since the reaction rate is in the zero-order regime proportional to the square of the overall CB concentration, the intermediate representing the kinetic bottleneck must be derived from P and the dimeric CB species. We assume that the complex TB–CB consisting of the reaction product TB and CB could be this intermediate. Based on these conclusions, we propose the following formal kinetic scheme:

$$\mathrm{CB} + \mathrm{CB} \rightleftharpoons \mathrm{CB2} \quad k_{5a}, k_{-5a} \qquad \text{(R5a)}$$

$$\mathrm{P} + \mathrm{CB2} \longrightarrow \mathrm{TB{-}CB} \quad k_{6a} \qquad \text{(R6a)}$$

$$\mathrm{P} + \mathrm{TB{-}CB} \longrightarrow 2\mathrm{TB} \quad k_{7a} \qquad \text{(R7a)}$$

$$\mathrm{TB} + \mathrm{CB2} \longrightarrow \mathrm{TB{-}CB} + \mathrm{CB} \quad k_{8a} \qquad \text{(R8a)}$$

The formation of CB2 occurs in the equilibrium reaction (R5a). P forms in reaction (R6a) with CB2 the complex TB–CB, which reacts with P in the autocatalytic step (R7a) to two product molecules TB. Finally, TB and CB2 form TB–CB and CB in reaction (R8a).

Numerical integration

Eqns. (8) to (12) hold for the reaction rates of reactants, intermediates, and product.

$$d[CB]/dt = 2k_{-5a}[CB2] - 2k_{5a}[CB]^2 + k_{8a}[CB2][TB] \quad (8)$$

$$d[CB2]/dt = k_{5a}[CB]^2 - k_{-5a}[CB2] - k_{6a}[CB2][P] - k_{8a}[CB2][TB] \quad (9)$$

$$d[P]/dt = -k_{6a}[CB2][P] - k_{7a}[TB{-}CB][P] \quad (10)$$

$$d[TB{-}CB]/dt = k_{6a}[CB2][P] - k_{7a}[TB{-}CB][P] + k_{8a}[CB2][TB] \quad (11)$$

$$d[TB]/dt = 2k_{7a}[TB{-}CB][P] - k_{8a}[CB2][TB] \quad (12)$$

The balanced equations relating $[CB]_o$ and $[P]_o$ with the actual concentrations of the four different species derived from borane and pinacolone, are given by eqns. (13) and (14).

$$[CB]_o = [CB] + 2[CB2] + 2[TB{-}CB] + [TB] \quad (13)$$

$$[P]_o = [P] + [TB{-}CB] + [TB] \quad (14)$$

The following initial concentrations hold true for $t = 0$: $[TB]_i = 0$, $[TB{-}CB]_i = 0$. The relatively rapid initial reaction of P was considered by setting $[P]_i = [P]_o - \Delta[P]$. $[CB]_i$ and $[CB2]_i$ are calculated from $k_{5a}/k_{-5a} = [CB2]_i/[CB]_i^2$ and eqn. (13) at $t = 0$. The actual concentration of P is known at any time t of the reaction. The kinetics could be resolved, since the reaction was measured with varying [P] and $[CB]_o$. The system of differential eqns. (8) to (12) was solved by numerical integration considering the known initial concentrations and eqns. (13) and (14). The fit parameters k_{5a}, k_{-5a}, k_{6a}, k_{7a}, and k_{8a} were varied until the calculated decay of [P] matched the experimental decay. The whole set of experimental kinetic curves could be reproduced by this procedure with the following rate constants: $k_{5a} = (1.9 \pm 0.2) \times 10^{-6}$ dm^3 mol^{-1} s^{-1}, $k_{-5a} = (8.0 \pm 0.8) \times 10^{-4}$ s^{-1}, $k_{6a} = (9.5 \pm 1.5) \times 10^{-4}$ dm^3 mol^{-1} s^{-1}, $k_{7a} = (4.8 \pm 0.5) \times 10^{-2}$ dm^3 mol^{-1} s^{-1}, and $k_{8a} = (6.7 \pm 1.8) \times 10^{-3}$ dm^3 mol^{-1} s^{-1}. Fig. 7 shows the quality of the resulting fits which is remarkably good, if the complexity of the experimental kinetics is considered.

Mechanistic considerations

The successful simulation of the kinetics suggests the reality

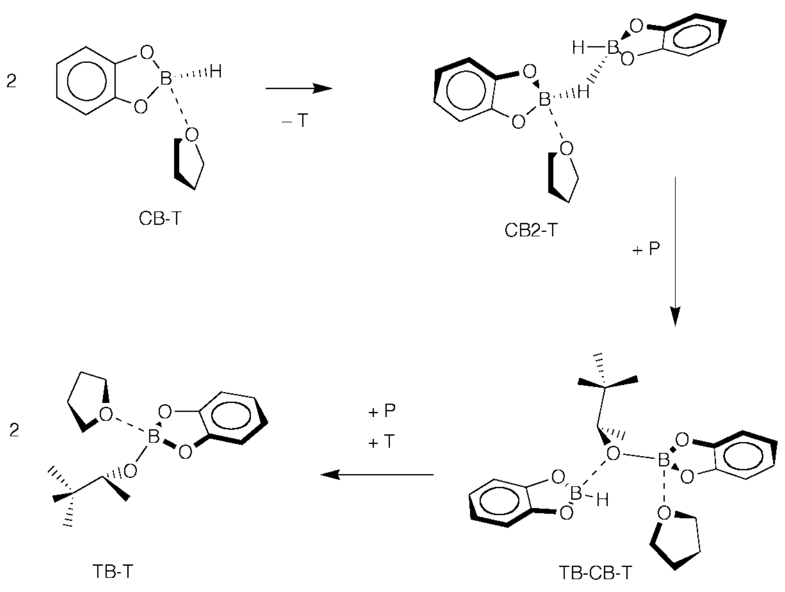

Scheme 2

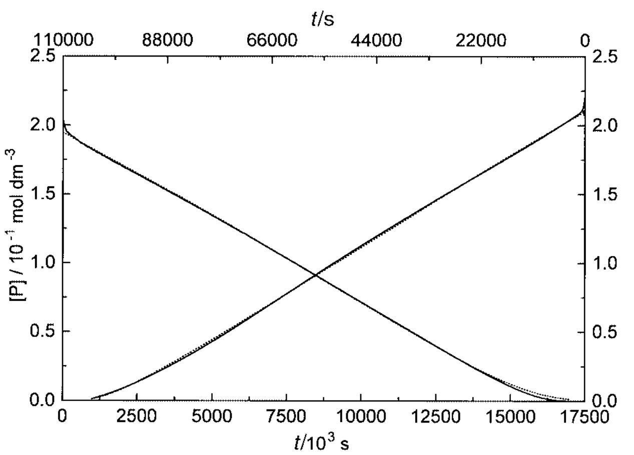

Fig. 7 Experimental and calculated kinetic curves. Solid curves represent experiment, dashed curves calculations. Concentrations in mol dm^{-3}, rate constant k_{-5a} in s^{-1}, rate constants k_{5a} to k_{8a} in dm^3 mol^{-1} s^{-1}. Lower timescale: $[\mathrm{CB}]_o = 3.5$, $k_{5a} = 2.1 \times 10^{-6}$, $k_{-5a} = 8.5 \times 10^{-4}$, $k_{6a} = 1.1 \times 10^{-3}$, $k_{7a} = 6.0 \times 10^{-2}$, $k_{8a} = 6.7 \times 10^{-3}$. Upper reversed timescale: $[\mathrm{CB}]_o = 1.5$, $k_{5a} = 2.0 \times 10^{-6}$, $k_{-5a} = 7.2 \times 10^{-4}$, $k_{6a} = 0.8 \times 10^{-3}$, $k_{7a} = 4.0 \times 10^{-2}$, $k_{8a} = 6.0 \times 10^{-3}$.

of the intermediates postulated in the kinetic scheme. To determine their possible structure and stability we performed semi-empirical calculations with AM1 parametrization. The heats of formation H^F calculated for optimized structures of minimum energy are given in Table 2. According to these calculations CB and THF form with the reaction enthalpy of $\Delta H = -27$ kJ mol^{-1} the complex CB–T, where the oxygen of THF coordinates with the CB boron, see Scheme 2.

A catecholborane dimer seems only to be stable, if it is coordinated with one THF molecule, whereby the CB–T moiety is bound to CB *via* one three center B–H–B bond. $\Delta H = -4$ kJ mol^{-1} is calculated for the formation of the dimer CB2–T from CB–T and CB. A stable structure is also obtained for the complex of TB–CB, if it is coordinated with one THF molecule. $\Delta H = -13$ kJ mol^{-1} results for the formation of TB–CB–T from TB–CB and THF. In TB–CB–T the oxygen atom of the alkoxy group of TB is bound to the boron of CB, whereas the neighboring boron atom of TB coordinates with the oxygen atom of THF. Finally also the product TB (= 2-(2-*tert*-butylethoxy)-1,3,2-benzodioxaborole) coordinates with THF forming TB–T with $\Delta H = -15$ kJ mol^{-1}, whereby the boron atom of TB coordinates with the oxygen atom of THF. Thus, the postulated intermediates, which are given in Scheme 2, could actually be realistic.

Considering the complexation with THF the kinetic scheme changes and is represented by reactions (R5) to (R8).

$$\text{CB–T} + \text{CB–T} \rightleftharpoons \text{CB2–T} + \text{T} \quad k_5, k_{-5} \qquad \text{(R5)}$$

$$\text{P} + \text{CB2–T} \longrightarrow \text{TB–CB–T} \quad k_6 \qquad \text{(R6)}$$

$$\text{P} + \text{T} + \text{TB–CB–T} \longrightarrow 2\text{TB–T} \quad k_7 \qquad \text{(R7)}$$

$$\text{TB–T} + \text{CB2–T} \longrightarrow \text{TB–CB–T} + \text{CB–T} \quad k_8 \qquad \text{(R8)}$$

Taking the molarity of the solvent $[\mathrm{T}] = 12.3$ mol dm^{-3} as constant, we finally obtain $k_5 = k_{5a}$, $k_{-5} = k_{-5a}/[\mathrm{T}] = (6.5 \pm 0.6) \times 10^{-5}$ dm^3 mol^{-1} s^{-1}, $k_6 = k_{6a}$, $k_7 = k_{7a}/[\mathrm{T}] = (3.9 \pm 0.4) \times 10^{-3}$ dm^6 mol^{-2} s^{-1}, and $k_8 = k_{8a}$.

Reaction (R5) with equilibrium constant $K_5 = k_5/k_{-5} = (3.0 \pm 0.3) \times 10^{-2}$ allows for the presence of dimeric CB species and thus for the reaction order of two in CB. However, the concentration of the dimeric CB is small. At $[\mathrm{CB–T}]_o = 0.5$ mol dm^{-3} the maximum concentration of CB2–T is calculated to be only 6.2×10^{-4} mol dm^{-3}. The reaction order of two in CB and the slowness of the reaction indicates that the reactivity of the monomeric CB towards ketones must be very small. As a matter of fact, electron delocalization from the oxygens to the boron leads to a stabilization of CB. In this respect CB is similar to dialkoxyboranes, which are known to be almost unreactive towards ketones.[16,17,19] It was assumed that the slow step of the reaction could involve the species TB–CB–T. Actually, the formation of TB–CB–T takes place rather slowly in reactions (R6) and (R8), whereas its consumption in reaction (R7) is fast with the pseudo-second-order rate constant $k_{7a} = k_7[\mathrm{T}] = 4.8 \times 10^{-2}$ dm^3 mol^{-1} s^{-1}. The analysis of the numerical integration demonstrates that in consequence [TB–CB–T] is very small but increases during the course of the reactions. For example, [TB–CB–T] increases from 1.4×10^{-3} to 1.3×10^{-2} mol dm^{-3} for the reaction with $[\mathrm{CB–T}]_o = 3.5$ mol dm^{-3} shown in Fig. 7. Since in the same time [P] decreases from about 0.20 to 0.02 mol dm^{-3}, the reaction rate $r = -\mathrm{d}[\mathrm{P}]/\mathrm{d}t$ remains approximately constant, explaining the zero reaction order in P.

The temperature dependence of r, which has been investigated in the range from 15 to 35 °C, leads to the very small activation energy of $E_a = 14.6 \pm 1.5$ kJ mol^{-1}, which is by about

50 or 40 kJ mol^{-1} smaller than the activation energies of the reactions of P with B–D or B–T, respectively. The reason for that discrepancy lies in the different complexity of the reaction sequences. The main part of the overall reaction is determined for B–D and B–T by the reactions of the pure educts in reactions (R4) and (R1). In the case of the reaction sequence with CB, however, P is mainly consumed in reaction (R7), a reaction with the intermediate TB–CB–T, which itself is formed in reactions (R6) and (R8). Thus, the experimental activation energy is a complex composite of the activation energy of reaction (R7) with the reaction enthalpies of reaction (R6) and (R8). Since, according to AM1 calculations, reaction (R6) is exothermic with $\Delta H_7 = -95$ kJ mol^{-1} and since reaction (R8) is almost thermoneutral a rather small activation energy results for the overall reaction of P with CB.

Conclusions

The kinetics of the reduction of the ketone pinacolone in THF depends strongly on the borane reagent and its purity. Commercial B–T and B–D both give rise to different kinetics and a strongly enhanced reactivity towards the ketone compared with the purified reagents. The main reactions of purified B–T and B–D with P are first-order in P and in borane complex. The reactivity of B–D is by a factor of four smaller than the reactivity of B–T. The comparison of the results of semi-empirical calculations with the experimental findings suggests that the principal reaction, the formation of the monoalkoxyborane from ketone and B–D, proceeds as a sequence of three reaction steps. The first step is probably the rate determining: the nucleophilic substitution of D in the complex B–D by the ketone P. The reaction of the ketone with catecholborane proceeds much slower with very strange reaction kinetics. The reaction order is two in CB and zero in P. These results indicate that the reactivity of the monomeric CB towards ketones must be very small. The complex kinetics can be successfully simulated by numerical integration. The reactive species is a catecholborane dimer being present in low concentrations. The zero-order kinetics in ketone points to some autocatalytic character of the reaction. In fact, the product TB reacts with the dimeric CB species to form a complex, which rapidly converts the ketone to TB. The results of this study will be valuable for the interpretation of the kinetics of the oxazaborolidine catalyzed reduction of ketones by B–D and CB.

Experimental

Kinetic measurements

A computerized Hewlett-Packard HP 8452 A diode array spectrometer allowing 0.2 s as the shortest interval between two consecutive spectra was used for the observations. O_2-free and dry solutions of the purified reagents B–D and CB in THF were transparent above 280 and 312 nm, respectively. The consumption of P was followed spectrophotometrically at 304 (B–D) or 314 nm (C–B). A correction was applied for the slight absorption of the CB reaction products at 314 nm. Unless otherwise stated, all experiments were carried out at 20 °C in THF. Because of the aggressiveness of this solvent a special stopped-flow apparatus was developed and manufactured in our facilities. All parts consist of steel, Teflon, Kel-F or glass. The solutions were transferred from Schlenk-flasks into the storage syringes under Ar by means of Teflon transfers. Instead of a stop syringe a Teflon tube leading into a bottle which is open to air is mounted to the outlet of the observation chamber. This means that developing gas bubbles cannot build up pressure during the reaction, which would cause baseline shifts. The storage syringes were driven by gas pressure, the flow was stopped by an adjustable rod which also operates a trigger switch to start the observations by the spectrometer.

NMR spectra

Chemical shifts for NMR spectra are reported as δ in units of parts per million (ppm) downfield from trimethylsilane (δ 0.0) using either internal or external standards. All measurements were carried out on a Bruker AMX 400 NMR-spectrometer at room temperature. The substances were dissolved in tetrahydrofuran-d_8 (99.8% deuterated), the small remaining amount of undeuterated tetrahydrofuran was used as standard in the case of ^1H measurements (δ 1.7, singlet and δ 3.6 ppm, singlet). For the ^{11}B measurements $BF_3{\cdot}OEt_3$ in THF was used as external standard (δ 0 ppm, singlet).

Reagents

Pinacolone (P, 2,2-dimethylbutan-3-one) (Aldrich, 98%) was distilled under Ar into a Schlenk-flask containing 4 Å molecular sieves. THF (T) (Riedel-de-Haën, p.a., 99.9%, stabilized by 2,6-di-*tert*-butyl-4-methylphenol) was dried over Na–K pearls and distilled under Ar. Borane–dimethyl sulfide (Aldrich) was cleaned by vacuum transfer into a trap cooled by liquid nitrogen.[23] Catecholborane (CB, 1,3,2-benzodioxaborole, Aldrich, 98%) was distilled at 50 °C (50 Torr) under Ar. Hereby it was found that the commercial CB was contaminated with surprisingly large (up to 30 wt%) and varying amounts of a white solid material, which remained as residue after distillation. The concentration of both the borane reagents was determined repeatedly by gas volumetry. The handling of all reagents was carried out under Ar to prevent contact with water. ^1H-NMR spectrum of purified CB (400 MHz, THF-d_8) [CB] = 0.27 mol dm^{-3}: δ 7.25 (m, 2 H), 7.08 (m, 2 H), 3.5–5.5 (q, 1 H). [CB] = 6.54 mol dm^{-3}: δ 7.25 (m, 2 H), 7.08 (m, 2 H), 6.97 (s), 3.5–5.5 (q, 1 H), 2.2–3.3 (q). ^{11}B-NMR spectrum (128 MHz, THF-d_8) [CB] = 6.54 mol dm^{-3}: δ 32.5–23.0 (d, 1 B), 21.52 (s), −17.4–−21.0 (q).

Acknowledgements

Financial support by the Adolf Messer Stiftung and the Fonds der Chemischen Industrie is gratefully acknowledged. We thank the Chemetall GmbH for gifts of chemicals.

References

1 S. Itsuno, K. Ito, A. Hirao and S. J. Nakahame, *J. Chem. Soc., Chem. Commun.*, 1983, 469.
2 E. J. Corey, R. K. Bakshi and S. J. Shibata, *J. Am. Chem. Soc.*, 1987, **109**, 5551.
3 L. Deloux and M. Srebnik, *Chem. Rev.*, 1993, **93**, 763.
4 S. Wallbaum and J. Martens, *Tetrahedron: Asymmetry*, 1992, **3**, 1475.
5 A. Togni and L. M. Venanzi, *Angew. Chem., Int. Ed. Engl.*, 1994, **33**, 497.
6 E. J. Corey and C. J. Helal, *Angew. Chem.*, 1998, **110**, 2092.
7 H. Jockel and R. Schmidt, *J. Chem. Soc., Perkin Trans. 2*, 1997, 2719.
8 R. Schmidt, H. Jockel, H.-G. Schmalz and H. Jope, *J. Chem. Soc., Perkin Trans. 2*, 1997, 2725.
9 D. J. Mathre, A. S. Thompson, A. W. Douglas, K. Hoogsteen, J. D. Carroll, E. G. Corley and J. J. Grabowski, *J. Org. Chem.*, 1993, **58**, 2880.
10 M. Masui and T. Shioiri, *Synlett*, 1997, 273.
11 P. Pinho, D. Guijarro and P. G. Andersson, *Tetrahedron*, 1998, **54**, 7897.
12 E. J. Corey, J. O. Link and R. K. Bakshi, *Tetrahedron Lett.*, 1992, **33**, 7107.
13 E. J. Corey and C. J. Helal, *Tetrahedron Lett.*, 1993, **34**, 5227.
14 B. T. Cho and M. H. Ryu, *Bull. Korean Chem. Soc.*, 1994, **15**, 1027.
15 T. Fujisawa, Y. Onogawa and M. Shimizu, *Tetrahedron Lett.*, 1998, **39**, 6019.
16 H. C. Brown and B. C. S. Rao, *J. Am. Chem. Soc.*, 1960, **82**, 681.
17 J. D. Pasto and B. Lepeska, *J. Am. Chem. Soc.*, 1976, **98**, 1091.
18 H. C. Brown, *Hydroboration*, W. A. Benjamin Inc., New York, 1962, p. 18.
19 J. D. Pasto, V. Balasubramaniyan and P. W. Wojitkowski, *Inorg. Chem.*, 1969, **8**, 594.

20 HyperChem software package release 4.5, 1995, Hypercube, Inc., Waterloo, Ontario.
21 Gmelin Handbuch der Anorganischen Chemie, vol. 48 (Borverbindungen Teil 16), p. 8, Springer Verlag, Berlin, Heidelberg, New York, 1977.
22 Personal communication by Chemetall GmbH, Frankfurt/M., Germany.
23 C. S. Shiner, *J. Am. Chem. Soc.*, 1985, **107**, 7167.

Paper 9/03202I